

# Detection of lateral composition modulation in a $(\text{InAs})_n/(\text{GaAs})_n$ short period superlattice on InP by magnetoexciton spectroscopy

E. D. Jones<sup>a</sup>, J. Mirecki-Millunchick<sup>a</sup>, D. Follstaedt<sup>a</sup>, M. Hafich<sup>a</sup>, S. Lee<sup>a</sup>,  
J. Reno<sup>a</sup>, R. Twesten<sup>a</sup>, Y. Zhang<sup>b</sup>, and A. Mascarenhas<sup>b</sup>

a) Sandia National Laboratories, Albuquerque, NM 87185-0601, USA

b) National Energy Renewable Laboratory, Golden, CO 80401

RECEIVED  
MAR 17 1997  
OSTI

## ABSTRACT

An experimental signature for detecting spontaneous lateral composition modulation in a  $(\text{InAs})_n/(\text{GaAs})_n$  short period superlattice on a InP substrate based on magnetoexciton spectroscopy is presented. We find by aligning the magnetic field in three crystallographic directions, one parallel to and the other two perpendicular to the composition modulation direction, that the magnetoexciton shifts are anisotropic and are a good indicator for the presence of composition modulation

## 2. INTRODUCTION

Low-dimensional structures, such as quantum wires and dots, have the potential to revolutionize microelectronic and photonic devices. These types of structures are expected to have lower laser-threshold currents, wider modulation bandwidths, better temperature stability, etc. However, they have been problematic to manufacture due to limitations in post-growth processing. Alternatively, self-assembled structures that are arranged in quantum-size configurations during growth can be used to obtain high densities of quantum wires and dots. For example, deposition of short period superlattices (SPS) of III-V alloys have resulted in lateral composition modulation which produces quantum wire structures. The phenomenon of spontaneous composition modulation in semiconductors has received attention in the literature where recently, an up-to-date summary of theoretical considerations, growth conditions, microscopy studies, and device applications was published as a conference proceedings.<sup>1</sup> To date, the principle experimental verifications for composition modulation have consisted of transmission electron microscopy,<sup>1</sup> optical absorption,<sup>2</sup> and polarized photoluminescence techniques.<sup>3</sup> Recently, x-ray reciprocal space analysis has also proven to be a valuable diagnostic tool for the detection and measurement of composition modulation.<sup>4,5</sup>

Transmission electron microscopy (TEM) is a powerful diagnostic and in many instances is the definitive measurement for microstructural analysis. However, because of sample preparation requirements, the TEM measurement can be labor intensive. As stated above, the application of x-ray reciprocal space analysis (KMAP) for studying composition modulation is relatively new and offers a rapid tool for characterization of not only composition modulation, but also for measuring lattice constants, strain parameters, etc.<sup>4,5</sup> Polarized photoluminescence techniques relies on crystal-field splitting of the valence-bands caused by the lowering of the zincblende cubic-symmetry by composition modulation.<sup>3</sup> However, besides composition modulation, there are other situations which also lead to reducing the crystal-field symmetry and two are (1) strained epilayers due to lattice mismatch between the substrate and the deposited film giving rise to a energy splitting of the valence-band states, and (2) spontaneous ordering effects such as observed for MOCVD-grown InGaAs epilayers on InP which result in a CuPt-type crystal structure.<sup>6</sup>

In this paper we report a new diagnostic tool using an old technique, magnetoexciton spectroscopy, for the detection of spontaneous lateral composition modulation. Here the magnetoexciton shifts are studied for three orientations of the magnetic field with respect to the direction of the composition modulation, giving a relatively fast and unambiguous determination for the presence of composition modulation. The structure used to demonstrate the utility of magnetoexciton spectroscopy is an  $(\text{InAs})_n/(\text{GaAs})_n$  SPS on a InP substrate that has spontaneously formed a lateral superlattice, perpendicular to the growth direction. The microstructure was confirmed by cross-sectional TEM, high resolution electron microscopy, and also low-temperature polarized photoluminescence spectroscopy.

DISTRIBUTION OF THIS DOCUMENT IS UNLIMITED

MASTER

**DISCLAIMER**

**Portions of this document may be illegible in electronic image products. Images are produced from the best available original document.**

### 3. EXPERIMENTAL

The SPS (sample no. G1517) was grown on a n-type InP (001) substrate by molecular beam epitaxy. A 3.0  $\mu\text{m}$ -thick  $\text{In}_{0.5}\text{Ga}_{0.5}\text{As}$  buffer layer of was deposited on the InP substrate. A 150-period undoped  $(\text{InAs})_n/(\text{GaAs})_n$  SPS with  $n \approx 1$  monolayer (ML) was deposited on top of the InGaAs buffer. On top of the SPS layers, a 0.5  $\mu\text{m}$  cap layer of undoped  $\text{In}_{0.5}\text{Ga}_{0.5}\text{As}$  was grown. The growth temperature was 500C and the growth rate  $R \approx 0.8$  ML/s which was calibrated by reflection high energy electron diffraction. Double crystal x-ray diffraction measurements show that the resulting structure, buffer and SPS layers have a nominal indium concentration of 48%, indicating that the resulting SPS structure is under tension.

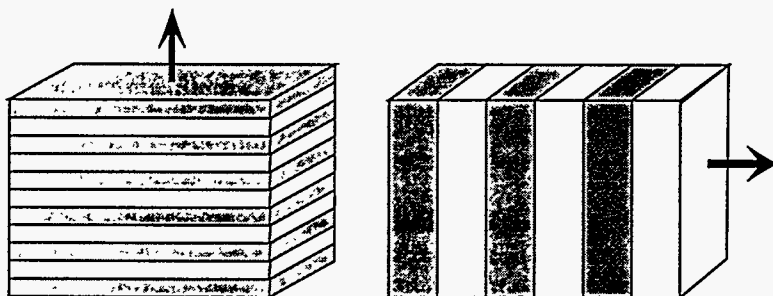


**Figure 1.** Schematic representation for the formation of a lateral composition modulated structure (right) from of a 1 ML SPS (left). The left arrow is the growth axis and the right is the lateral composition modulation direction

A schematic representation for the formation of lateral composition modulation from a SPS is shown in Fig 1. The left hand figure represents the as grown SPS structure and the right hand schematic is the resulting lateral composition modulation structure. The left arrow is the growth direction for the SPS and the right is the lateral composition modulation direction. The SPS period is about 1 ML and thus the graphic is not to scale. Typical wavelengths for composition modulation vary between 5 and 20 nm. High resolution TEM showed even after the formation of the composition modulation, that the SPS layers were still present with evidence of distortion of the layers.<sup>2</sup>

Two TEM images of this structure are shown in Fig. 2. The left side of the Fig. 1 shows the formation of the lateral composition modulation while the orthogonal direction shows a uniform distribution characteristic of a random alloy. The modulation wavelength  $\lambda$  is asymmetric and when averaged over the structure  $\lambda \approx 13$  nm. As can be seen in the figure, the composition modulation also is present in the buffer layer. At the present time, the root causes for composition modulation are currently being pursued, and hence the presence of the composition modulation in the buffer layer is not understood

The magnetoexciton spectroscopy measurements were made at 1.4 K and the magnetic field varied between 0 and 14T. The sample was attached to the end of a 100  $\mu\text{m}$ -core-diameter optical fiber and located in a variable temperature dewar (1.4 K  $\leq T \leq 300$  K) insert placed in the middle of the superconducting magnet. The sample-fiber combination could be oriented in the three principle magnetic field directions, i.e., magnetic field along the growth direction [001], magnetic field along the [110], and magnetic field along the  $[\bar{1}\bar{1}0]$  composition modulation direction. The PL measurements were made with an Argon-ion laser operating at 514.5 nm. The laser was injected into the optical fiber by means of a optical beam-splitter and the returning photoluminescence signal was directed to a 0.27-meter,  $f/4$  optical monochromator and a IEEE488-based data acquisition system. Typical laser power densities on the sample were of the order of 1 W/cm<sup>2</sup> and a NORTH COAST EO-817 germanium detector was used to detect the 1.6  $\mu\text{m}$  infrared energy photons.

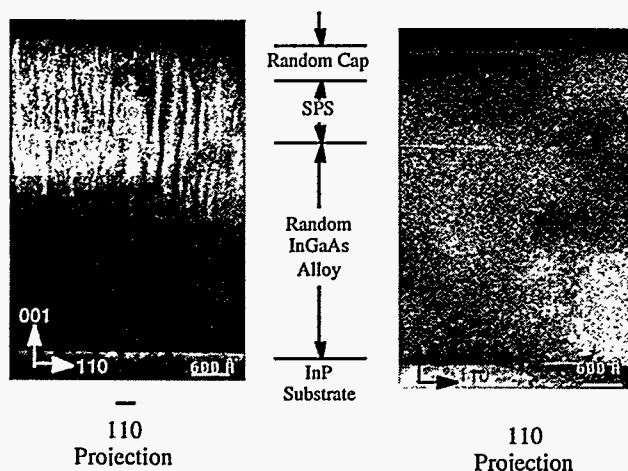


**Figure 2.** Dark field images of the  $(\text{InAs})_n/(\text{GaAs})_n$  SPS structure for the  $[\bar{1}\bar{1}0]$  and  $[110]$  projections. The left side of the figure shows the lateral contrast variation due to composition modulation in the  $[\bar{1}\bar{1}0]$  projection, but not in the orthogonal  $[110]$  projection shown on the right side. The average modulation wavelength over the sample is about 13 nm.

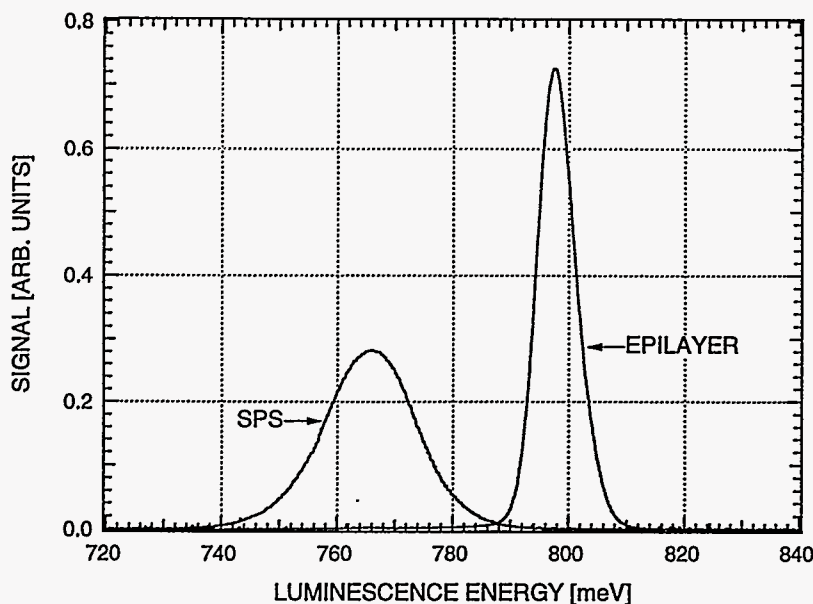


Figure 3. Two low-temperature zero-field PL spectra. The 1.4-K PL spectrum for the composition modulated SPS structure is shown on the left while on the right is a 4-K spectrum from an undoped, nominally lattice matched, epilayer of InGaAs/InP taken. The relative signal strengths of the two spectra are approximately correct.

Two zero-field PL spectra are shown in Fig 3. The 1.4-K PL spectrum for the composition modulated SPS structure is shown on the left while the right hand PL spectrum is that from an undoped, nominally lattice-matched, epilayer of InGaAs on InP (sample no. G1872) taken at 4K. The full-width-at-half-maximum (FWHM) of the composition modulated SPS structure is 18.5 meV and for the epilayer sample, FWHM  $\approx$  8meV. The indicated relative signal strengths of the two spectra with are approximately correct. Neglecting strain effects, the 1.4-K bandgap energy of  $E_g \approx 762$  meV for the SPS sample is considerably lower than the expected bandgap energy  $E_g$  of about 870 meV for an  $\text{In}_{0.48}\text{Ga}_{0.52}\text{As}$  alloy. A bandgap reduction of nearly 100 meV may be a measure of the presence of strong composition modulation, however, until the actual shape, composition modulation amplitude, valence-band offsets, etc., of the composition modulated region is known, it is difficult to make quantitative interpretations. The epilayer's PL spectrum peak energy of 798 meV is also somewhat lower than the accepted bandgap energy of 812 meV for lattice matched InGaAs/InP epilayer. The energy difference between the accepted lattice matched bandgap energy of  $E_g = 812$  meV and the observed 798 meV may be attributed to small composition differences. A general rule of thumb for the InGaAs ternary alloys system nominally lattice matched to InP is a change to the bandgap energy  $\Delta E_g$  of about 12 meV per percent change in composition. Nominally lattice-matched InGaAs epilayers on InP substrates grown at various times and under varying conditions in our laboratories show exciton-peak energies ranging from 790 to 820 meV. Double crystal x-ray diffraction measurements of the lattice constant, and hence composition, for these other epilayer specimens, also show a similar variation.

#### 4. MAGNETOEXCITONS

In undoped semiconductors, the coulomb interaction between conduction-band electron and a valence-band hole can form a hydrogenic type bound state which is referred to as an exciton. The observed magnetoexciton diamagnetic shifts can be fitted using a simple hydrogenic model and from first-order perturbation calculations, the diamagnetic shift of the 1s ground state is given by, in cgs units,

$$\Delta E = \frac{1}{2} R^* \gamma^2, \quad (1)$$

where  $\gamma = (\hbar\omega_c / 2R^*)$ ,  $\hbar\omega_c = (2\mu_B B / \mu c)$  is the cyclotron resonance energy,  $R^* = (\mu e^4 / 2\hbar^2 \epsilon^2)$  is the effective rydberg,  $\hbar$  is Plank's constant over  $2\pi$ ,  $\mu$  is the reduced mass ( $1/\mu = 1/m_c + 1/m_v$ ),  $m_c$  and  $m_v$  are the conduction and valence-band masses,  $\epsilon$  is the static dielectric constant,  $\mu_B$  is the Bohr magneton,  $c$  is the velocity of light, and  $B$  is the applied magnetic field. Combining all of the above, the magnetoexciton diamagnetic shift  $\Delta E$  given in Eq. (1) depends upon the reduced mass  $\mu$  and magnetic field  $B$  in the following manner  $\Delta E \propto \mu^{-3} B^2$ , i.e., quadratic in magnetic field and inversely proportional to the cube-power of the reduced mass.

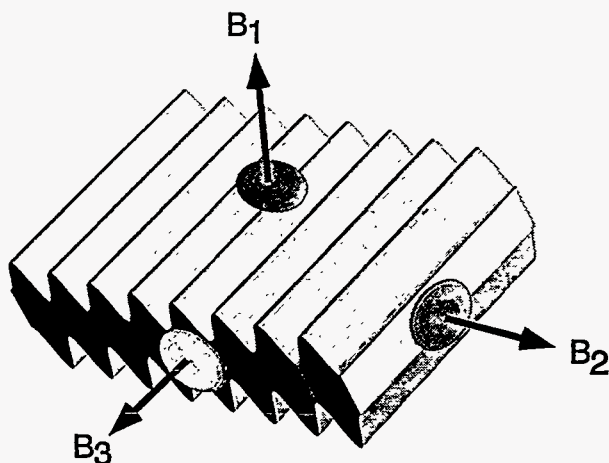


Figure 4. Schematic drawing showing the spatial dependence of the bandgap energy resulting from the  $\lambda = 13\text{nm}$  composition modulation wave and. The three principle directions for the magnetic field are  $B_1$ ,  $B_2$ , and  $B_3$ . The “donut” or “button” shapes represent the plane for the exciton orbits in the magnetic field.

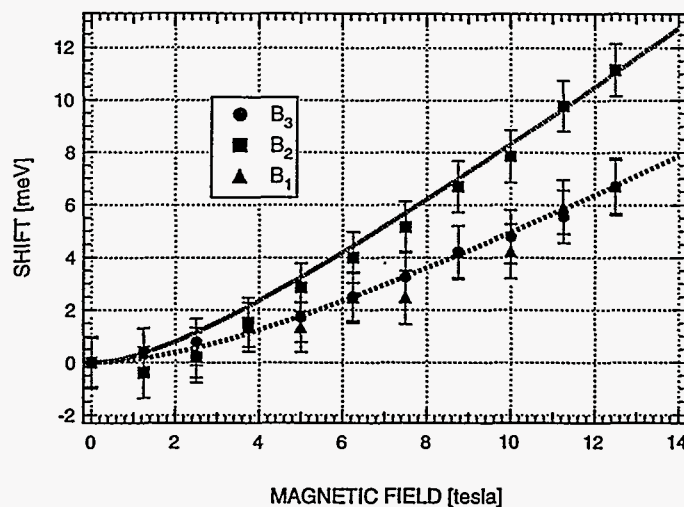


Figure 5. Diamagnetic shifts for composition modulated SPS structure. The three directions of the magnetic field are indicated as  $B_1$ ,  $B_2$ , and  $B_3$  and correspond to the same alignments as shown in Fig. 4. The lines are best fit curves of Eq. (1) to the data for the three magnetic field orientations and  $\mu(B_2) = 0.042m_0$  and  $\mu(B_1) = \mu(B_3) = 0.056m_0$ .

## 5. DISCUSSION

The experiment is thus performed by measuring the exciton diamagnetic shift, Eq. (1), in the three principle directions, i.e., along the growth axis, and two orientations perpendicular to the growth axis; (1) magnetic field along the composition modulation direction and (2) magnetic field perpendicular to the composition modulation direction. A schematic for these orientations is shown in Fig. 4, where a three dimensional view of the bandgap energy associated with the composition modulation wave is shown as a spatially varying amplitude. The orientation  $B_1$  is along the growth axis,  $B_2$  is along the composition modulation direction, and  $B_3$  is perpendicular to both the growth and composition modulation directions. The plane of exciton orbits for the three directions are the “donut” or “button” shapes shown for each magnetic field orientation. Because the zero-field exciton radius for InGaAs/InP is nearly  $200 \text{ \AA}$ , the exciton orbits for two of the orientations, namely along the two perpendicular directions to the  $\lambda = 130 \text{ \AA}$  composition modulation wave, will include areas of varying composition and hence areas of varying bandgap energies. As is obvious from Fig. 4, the only orientation where the plane of the exciton orbit remains in a non-varying composition region (non-varying bandgap energy) is the  $B_2$  direction.

Figure 5 shows the magnetoexciton diamagnetic shifts taken for the three principle directions  $B_1$ ,  $B_2$ , and  $B_3$  at a temperature of 1.4K. As one can see from the figure, the diamagnetic shift for two directions,  $B_1$  and  $B_3$ , are nearly identical while the diamagnetic shift for the  $B_2$  direction is about 50% larger than the other two orientations. The lines drawn through the data are best fits of Eq. (1), with  $k \approx 12.8$ , with the result  $\mu(B_2) = 0.042m_0$  and  $\mu(B_1) = \mu(B_3) = 0.056m_0$ , where  $m_0$  is the free electron mass. The conduction-band mass for lattice-matched InGaAs/InP is generally accepted to be  $0.04m_0$ , indicating that the valence-band mass is large. A large valence-band mass can arise from bulk-band behavior where the two “heavy-hole” and “light-hole” valence-bands are degenerate, or from the valence-band energy levels under tension. The former explanation for a heavy-hole mass contribution to the reduced exciton mass  $\mu$  is possibly the more correct assumption, especially in view of the optical absorption data obtained by Roura et. al.,<sup>2</sup> who suggest that the maximum variation in their composition modulation samples is no more than 1.2% or using our general-rule-of-thumb, the maximum bandgap energy variation would be about 14 meV. If the variation to the reduced mass of  $0.042m_0$  to  $0.056m_0$  is entirely due to the conduction band electrons, than one can perform the following analysis about the change in composition. The conduction band-masses for InAs and GaAs are respectively  $0.023m_0$  and  $0.067m_0$ . Assuming a linear variation for the conduction-band mass between InAs and GaAs predicts a change in mass of  $\delta\mu = 4.4 \times 10^{-4}$  per percent change in composition. Using this linear extrapolation value, the lattice matched  $\text{In}_{0.54}\text{Ga}_{0.46}\text{As/InP}$  mass is  $0.047m_0$  which is reasonable in view of the mass uncertainties. Thus the  $0.014m_0$  mass difference between the three orientations suggest a 31% change in composition which is an unacceptably

large value. Thus until the exact nature of the energy band structure for these kinds of materials can be quantified, we will not be able to make quantitative analyses about the composition modulation wave. However, the qualitative nature of the anisotropic diamagnetic magnetoexciton shifts does provide a good signature for the presence of composition modulation.

One final comment concerns the size of the diamagnetic shift. In Fig. 5, the size of the exciton diamagnetic shift in the  $B_1$  orientation is about 7 meV and for the  $B_2$  orientation it is about 12 meV. For comparison, the diamagnetic shift for a bulk InGaAs epilayer on InP is nearly 13 meV at our maximum magnetic field. Thus, we see that (1) the maximum shift in the  $B_2$  directions is somewhat smaller than the bulk epilayer, indicating some quantum confinement, and (2) the diamagnetic shift in the normal direction ( $B_1$ ) is about 60% of the bulk diamagnetic shift. Thus a single measurement in the  $B_1$  direction will provide a quick determination for the presence of composition modulation. If the diamagnetic shift is nearly that of the bulk value, then in all probability, the composition modulation, if present, is weak.

In conclusion, we have shown that by performing magnetoexciton spectroscopy in three different directions can provide another diagnostic tool for the presence of composition modulation. When more detail concerning the size, shape, etc., of the composition modulation region becomes available, then these kinds of studies will provide more insight about the local bandstructure properties.

## 6. ACKNOWLEDGMENTS

The authors wish to thank Dr. S. K. Lyo for providing the magnetoexciton diamagnetic shift program for fitting the data. This work was supported in part by the Division of Material Science, Office of Basic Energy Science, U. S. DOE, No. DE-AC04-94AL8500.

## REFERENCES

1. Optoelectronic Materials - Ordering, Composition Modulation, and Self-Assembled Structures, Edited by E. D. Jones, A. Mascarenhas, and P. Petroff, Volume 417, Materials Research Society Symposium Proceedings, Pittsburgh, 1996.
2. P. Roura, J. Bosch, S. A. Clark, F. Peiró, A. Cornet, J. R. Morante, and R. H. Williams, "Quantification by optical absorption of the coarse modulation observed by transmission electron microscopy in InGaAs layers grown on InP(100)", *Semicond. Sci. Technol.* **11**, 1310 - 1316 (1996).
3. A. Mascarenhas, R. G. Alonso, G. S. Horner, S. Froyen, K. C. Hsieh, and K. Y. Cheng, "Experimental evidence for a spontaneously generated effective mass lateral superlattice", *Superlattices and Microstructures* **12**, 57 - 61, (1992).
4. S.R. Lee, B.L. Doyle, T.J. Drummond, J.W. Medernach and R.P. Schneider, Jr., "Reciprocal Space Mapping of Epitaxial Materials Using Position-Sensitive X-ray Detection," *Advances in X-ray Analysis*, Volume 38, Edited by: Paul K. Predecki et al., Plenum Press, New York, 1995.
5. J. Mirecki Millunchick, R. D. Twisten, D. M. Follstaedt, S. R. Lee, E. D. Jones, Y. Zhang, S. P. Ahrenkiel, and A. Mascarenhas, "Composition modulation in AlAs/InAs short period superlattices grown on InP(001)," accepted for publication, *Appl. Phys. Lett.* (1997).
6. S. P. Ahrenkiel, R. K. Ahrenkiel, and D. J. Arent, "Domain structure and transient photoconductivity in ordered  $Ga_{0.47}In_{0.53}As$  epitaxial films", *Proceedings of the Fall 1996 Materials Research Conference*.